Reduced order modeling of large contact interfaces to calculate the non-linear response of frictionally damped structures

Available online at www.sciencedirect.com

ScienceDirect

Procedia Structural Integrity 24 (2019) 837–851

Structural Integrity Procedia

www.elsevier.com/locate/procedia

AIAS 2019 International Conference on Stress Analysis

# Reduced order modeling of large contact interfaces to calculate the non-linear response of frictionally damped structures

G. Battiato[a,*], C. M. Firrone[a]

[a]*Politecnico di Torino, Corso Duca degli Abruzzi 24, Torino 10129, Italy*

**Abstract**

The design of complex structures requires a deep understanding on how neighboring components mutually interact during vibration. Such interaction makes the dynamic behavior of the whole system highly nonlinear due to the presence of contact phenomena at the interfaces between the components. Although several mechanical applications exhibit localized friction joints, a wide variety of structures involve a class of joints featuring extended contact interfaces. This is the case of bolted flanges and lap joints used in turbomachinery for aeronautical applications. Modeling the dynamics of such large structures by using commercial FE codes is the typical approach that industries would adopt. However, two issues must be faced at the same time. First, the number of degrees of freedom involved in the numerical simulation is sometimes so large that even linear dynamic analyses become prohibitive in terms of required computational time or limited capabilities of the computer hardware. Second, the non-linear behavior of frictional joints can only be evaluated by direct time integration approaches, making most of the time the analyses unfeasible due to huge computational costs. This paper addresses both aspects together by proposing novel techniques for the modal reduction of FE models, which guarantee high compression of the number of the degrees of freedom at the contact interfaces. This allows for a modal representation of the corresponding contact forces by leading to a dramatic reduction of the size of the non-linear problem.



*Keywords:* Type your keywords here, separated by semicolons ;

* Corresponding author. Tel.: +39-011-090-6953
*E-mail address:* giuseppe.battiato@polito.it


10.1016/j.prostr.2020.02.074

## 1. Introduction

The design of an aircraft engine is a complex iterative process aimed at achieving the best compromise between aerodynamic and structural requirements. A deep understanding on how mechanical components behave from both a static and dynamic point of view is therefore necessary in order to optimize the system performance by increasing the efficiency. In aircraft engines and specifically in low pressure turbine bladed disks both mechanical and unsteady aerodynamic loads are the main responsible for *high cycle fatigue* (HCF), which is considered the "major cost, safety and reliability issue for gas turbine engine" (Castanier et al. (2006)). For this reason blades and disks require special attention and a very careful design due to the crucial role they play during the operation of gas turbine engines. As so much is dependent on the reliability of these components, the tendency of manufacturers would be to over-design them in order to largely cope the safety specifications. On the other , limited weights are necessary to achieve the high efficiency characterizing the latest generation gas turbine engines. This aspect unavoidably leads to design much slender blades and thinner disks, making them more prone to mechanical vibrations.

Due to the large operative range characterizing these systems, bladed disks can not be designed to work outside of all resonant zones. Their configuration comes from preliminary aerodynamic and efficiency considerations which make the design strict and not easily modifiable. This statements can be easily visualized by looking at the schematic *Campbell / Waterfall* diagram of a turbine bladed disks (Fig. 1):

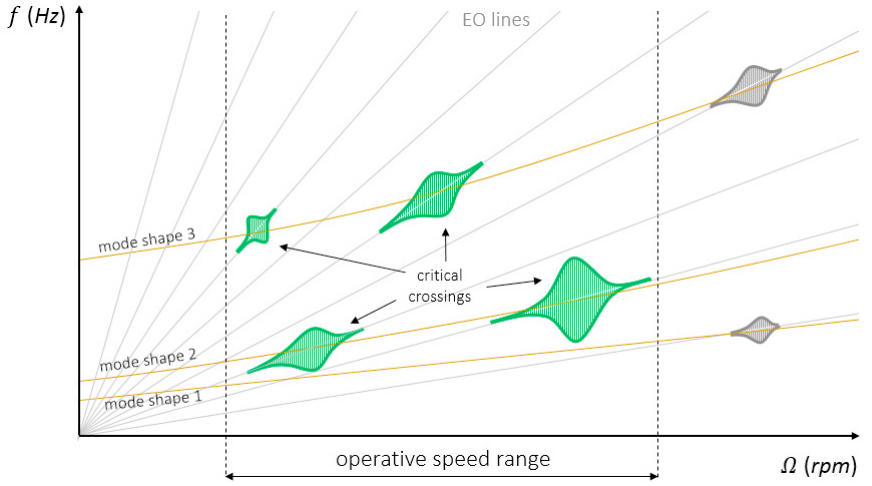


Fig. 1. *Campbell / Waterfall* diagram of a turbine bladed disks: the disk's natural frequencies are here plotted as a nearly horizontal lines whose actual shape depends on the rotor speed Ω. This is due to the blades' stiffening effect caused by the increasing centrifugal force. The straight lines starting from the axis origin denote the so called *engine order* (EO) traveling wave excitation and represent the harmonic content of the unsteady pressure distribution exciting the bladed disk.

Among all the possible crossings between the mode shapes and the EO lines, just few of them actually correspond to resonance conditions. In particular, the critical crossings are those for which the relationship holds:

$$EO = z \cdot N \pm H, \qquad \forall\, z \in \mathbb{N}^* \tag{1}$$

where $N$ is the number of disk's sectors (i.e. the number of blades) and $H$ is the harmonic index of the mode shape, i.e. the number of nodal diameters occurring during the vibration (Battiato et al. (2018)). Although some critical crossings can be "moved" outside the operative range by slightly modifying the disk design (grey resonances in Fig. 1), some others can not be avoided and additional sources of damping are necessary to mitigate the effects of dangerous vibrations. This practice is crucial to avoid unacceptable level of dynamic stresses that would drastically reduce the fatigue life of the most critical engine's components (e.g. the blades).

Nowadays, the most used practices to reduce dynamic stresses in bladed disks would be exploiting *dry friction* occurring at the joints used to connect the engine's components. These might involve specific blade's locations (blade root,shroud, part span shroud) (Zucca et al. (2012); Krack et al. (2013)) or the employment of external devices known as *friction dampers* (underplatformdampers, snubbers) (Sanliturk et al. (2001); Petrov et al. (2007); Firrone et al. (2013); Schwingshackl et al. (2012)). However, simulating the damping effect caused by such localized joints is of interest especially when studying forced vibrations of single bladed disks assemblies.

In order to meet the needs of industries the scientific community is now moving towards the dynamic analysis of the effects that extended joints have on large structural systems. In the field of turbomachineries typical examples are the multi-stage bladed disks connected by bolted flanges (Battiato et al. (2018)) and the casing-vanes assemblies where extended lap joints can be found (Lassalle et al. (2016)). The mentioned trend comes up beside another relevant task, that is the development of advanced numerical techniques in order to make the prediction of the non-linear forced response of these structure feasible and efficient. This would overcome the limited practices currently used by industries which require modeling the mechanical systems by using commercial FE codes. However, due to the increasing complexity of the mechanical components and the need to simulate larger structures, two issues must be faced at the same time. First, the number of degrees of freedom (DoFs) involved in the numerical simulation is sometimes so large that even linear dynamic analyses become prohibitive in terms of computational time or limited capabilities of the computer hardware. Second, in FE codes the non-linear behavior of frictional joints can only be evaluated by direct time integration approaches, which makes most of the time the analyses unfeasible due to huge computational costs. This paper addresses both aspects by presenting novel techniques for the modal reduction of FE models that guarantee high compression of the number of non-linear DoFs at the contact interfaces. This allows for a modal representation of the corresponding contact forces by leading to a dramatic reduction of the size of the non-linear problem to be solved. The goodness of the proposed methodologies is quantified both in terms of accuracy and time costs savings on the calculation of non-linear forced response by using the Harmonic Balance Method (HBM).

## 2. Non-linear forced response analysis

In this section the equations of motion (EQM) of a structure with contact interfaces are introduced and the solution strategy based on the HMB (Cardona et al. (2016)) is presented.

Solving complex dynamic and static structural problems often requires modeling the mechanical components by using the FE method. Design practices in industries are in fact based on the usage of robust FE codes. At the same time even commercial FE codes are even largely employed in academia to carry out research projects. For these reasons the following description of non-linear dynamic systems requires the definition of matrix and vector quantities that can either be just exported from commercial FE software or further processed by suitably defined reduction techniques (see section 3).

The EQM of a large structural system with contact interfaces can be written as:

$$\mathbf{M}\ddot{\mathbf{x}}(t) + \mathbf{C}\dot{\mathbf{x}}(t) + \mathbf{K}\mathbf{x}(t) = \mathbf{f}_e(t) - \mathbf{f}_c(\mathbf{x}, \dot{\mathbf{x}}, t) \tag{2}$$

where $\mathbf{M}$, $\mathbf{C}$ and $\mathbf{K}$ are the mass, viscous damping and stiffness matrices, $\mathbf{x}(t)$ is the vector of generalized DoFs, while $\mathbf{f}_e(t)$ and $\mathbf{f}_c(\mathbf{x}, \dot{\mathbf{x}}, t)$ are the corresponding vectors of external and non-linear contact forces respectively. Note that $\mathbf{x}(t)$ contains just physical DoFs if FE matrices are used, while it collects a mix of physical and modal coordinates when particular *component mode synthesis* reduction schemes are used (Gruber et al. (2016)).

In order to reduce the large calculation times typical of the numerical integration of non-linear systems, the HBM can be used to compute the steady-state response of the system. In particular, due to the periodicity of $\mathbf{f}_e$, the displacements $\mathbf{x}$ and the non-linear contact forces $\mathbf{f}_c(\mathbf{x}, \dot{\mathbf{x}}, t)$ are periodical at steady-state. These quantities can then be written

as the real part of the following truncated series of harmonic terms:

$$\mathbf{x}(t) = \sum_{h=0}^{N_h} \mathbf{X}^{(h)} \cdot e^{ih\omega t}, \qquad \mathbf{f}_n(\mathbf{x}, \dot{\mathbf{x}}, t) = \sum_{h=0}^{N_h} \mathbf{F}_c^{(h)} \cdot e^{ih\omega t} \tag{3}$$

where $\mathbf{X}^{(h)}$ and $\mathbf{F}_c^{(h)}$ are the $h^{th}$ order complex amplitudes of the displacements and contact forces respectively, $\omega$ is the circular frequency and $N_h$ is the number of retained harmonics required by the HBM approximation. By plugging Eqn. 3 into Eqn. 2, the EQM are turned into a set of non-linear, complex, algebraic equations:

$$\mathbf{D}^{(h)}(\omega)\mathbf{X}^{(h)} = \mathbf{F}_e^{(h)} - \mathbf{F}_c^{(h)}, \qquad \forall\, h = 0, \ldots, N_h \tag{4}$$

where $\mathbf{D}^{(h)}(\omega) = \mathbf{K} + ih\omega\mathbf{C} - (h\omega)^2\mathbf{M}$ is the $h^{th}$ order dynamic stiffness matrix.

Since non-linear contact forces $\mathbf{f}_c$[1] only depend on the relative displacements of the contact DoFs, it would be convenient to rearrange Eqn. 4 in order to decouple the solution of the non-linear part of the problem from the linear one. A possible strategy to accomplish this task requires the evaluation of the receptance matrix $\mathbf{H}^{(h)}$ (i.e. the inverse of $\mathbf{D}^{(h)}$), so that the EQM can be re-written in the following form:

$$\mathbf{X}^{(h)} = \mathbf{X}_e^{(h)} - \mathbf{H}^{(h)}\mathbf{F}_c^{(h)}, \qquad \forall\, h = 0, \ldots, N_h \tag{5}$$

The first term at the right-hand side of Eqn. 5 represents the steady-state linear response of the structure due to the external excitation (i.e. $\mathbf{X}_e^{(h)} = \mathbf{H}^{(h)}\mathbf{F}_e^{(h)}$), while the second term takes into account the contribution of the non-linear forces. In order to distinguish the non-linear partition from the linear one, the vectors $\mathbf{X}^{(h)}$, $\mathbf{F}_e^{(h)}$ and $\mathbf{F}_c^{(h)}$ can be written as:

$$\mathbf{X}^{(h)} = \begin{Bmatrix} \mathbf{X}_n^{(h)} \\ \mathbf{X}_l^{(h)} \end{Bmatrix}, \qquad \mathbf{F}_e^{(h)} = \begin{Bmatrix} \mathbf{F}_{e,n}^{(h)} \\ \mathbf{F}_{e,l}^{(h)} \end{Bmatrix}, \qquad \mathbf{F}_c^{(h)} = \begin{Bmatrix} \mathbf{F}_{c,n}^{(h)} \\ \mathbf{F}_{c,l}^{(h)} \end{Bmatrix} \tag{6}$$

where the subscripts $n$ and $l$ denote the non-linear (contact) and linear DoFs respectively. By using the partitioning of Eqn. 6, Eqn. 5 becomes:

$$\begin{Bmatrix} \mathbf{X}_n^{(h)} \\ \mathbf{X}_l^{(h)} \end{Bmatrix} = \begin{Bmatrix} \mathbf{X}_{e,n}^{(h)} \\ \mathbf{X}_{e,l}^{(h)} \end{Bmatrix} - \begin{bmatrix} \mathbf{H}_{nn}^{(h)} & \mathbf{H}_{nl}^{(h)} \\ \mathbf{H}_{ln}^{(h)} & \mathbf{H}_{ll}^{(h)} \end{bmatrix} \begin{Bmatrix} \mathbf{F}_{c,n}^{(h)} \\ \mathbf{F}_{c,l}^{(h)} \end{Bmatrix} \tag{7}$$

where the quantity $\mathbf{F}_{c,l}^{(h)}$ is assumed to be equal to the zero vector since the non-linear contact forces only depend on the non-linear displacements. Therefore, the non-linear partition of the EQM is represented by the following set of matrix equations:

$$\mathbf{X}_n^{(h)} = \mathbf{X}_{e,n}^{(h)} - \mathbf{H}_{nn}^{(h)}\mathbf{F}_{c,n}^{(h)}, \qquad \forall\, h = 0, \ldots, N_h \tag{8}$$

[1] In order to simplify the notation the explicit dependency of the vector quantities on the relative displacements and time is hereafter removed.

Such set of equations is non-linear and has to be solved for the complex amplitudes of the contact DoFs by using an iterative solution method (e.g. Newton-Raphson algorithm). Once the non-linear forces $\mathbf{F}_{c,n}^{(h)}$ are obtained from Eqn. 8, the response of the linear DoFs $\mathbf{X}_{l}^{(h)}$ can be found by solving the following equation:

$$\mathbf{X}_{l}^{(h)} = \mathbf{X}_{e,l}^{(h)} - \mathbf{H}_{ln}^{(h)}\mathbf{F}_{c,n}^{(h)} \tag{9}$$

It must be noted that the equations of Eqn. 8 are coupled to each other, meaning that the harmonic components of the non-linear contact forces $\mathbf{F}_{c,n}^{(h)}$ depend on all the harmonic components of the non-linear displacements $\boldsymbol{X}_{n}^{(h)}$.

### 2.1. Contact forces evaluation

The problem of modeling periodical contact forces due to friction contacts and their implementation in numerical solvers has been addressed by several authors. The commonest method found in literature for the calculation of the non-linear forced response is based on the so called *Alternating Frequency Time* (AFT) method (Cameron et al. (1989); Poudou et al. (2003)). This method requires to evaluate the contact forces in the time domain by using the contact model that better describes the actual contact state at the interface between the interacting components (Firrone et al. (2011)). Among the contact models found in the technical literature the most used is the 1-D contact element with normal load variation (Yang et al. (1998)) (Fig. 3).

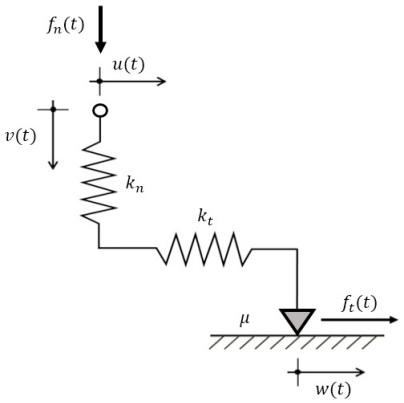


Fig. 2. 1-D contact element with normal load variation.

In Fig. 3 $u(t)$ and $v(t)$ represent the tangential and normal relative displacement defined by two nodes in contact, while $w(t)$ is the tangential displacement of the slider. The contact model's parameters are represented by the tangential and normal contact stiffnesses, $k_t$ and $k_n$ respectively, the coefficient of friction $\mu$ and the normal preload $f_0$. The normal contact force $f_n(t)$ is defined as:

$$f_n = \max(f_0 + k_n \cdot v(t), 0) \tag{10}$$

while the tangential contact force $f_t(t)$ depends on the contact state, i.e. stick, slip and lift-off. For each of these the contact force in the tangential direction can be written as:

$$f_t = \begin{cases} k_t \cdot u(t) & \text{stick} \\ \text{sgn}(\dot{w}) \cdot \mu f_n & \text{slip} \\ 0 & \text{lift-off} \end{cases} \tag{11}$$

## 3. Interface reduction methods

The prediction of the effects that friction has on the non-linear response of structures with large contact interfaces is a crucial task for industries. The major challenge comes from the difficulty of ling detailed FE models with highly refined meshes at the contact interfaces. From a mathematical point of view this means having the non-linear partition of Eqn. 7 not negligible with respect the linear one (i.e. $\dim(\mathbf{X}_n^{(h)}) \not\ll \dim(\mathbf{X}_l^{(h)})$). Therefore, using the 1-D Jenkins element for each pair of nodes in contact would be inconvenient if no reduction methods are applied to the contact interface DoFs.

The drawback of simulating contact on regions with a high density of DoFs is overcome by using interface reduction methods (Castanier et al. (2001); Holzwarth et al. (2015); Kuether et al. (2017)). These allow for a modal representation of the contact interfaces by achieving a dramatic compression on the number of DoFs. In this paper two novel interface reduction methods are presented, i.e. the *Gram-Schmidt interface* (GSI) method (Battiato et al. (1-2018, 2-2018)) and the *Multi-stage* (MS) method (Firrone et al. (2018); Battiato et al. (2018)). The first is more general and suitable for any geometry of the contact interfaces, while the second was specifically developed for interfaces featuring a circular geometry.

### 3.1. Reduction scheme for the contact interface

Regardless of the particular interface reduction method, the mathematical scheme used to modalize the interface DoFs is basically the same. Let us consider two mechanical components interacting to each other through an extended contact interface (Fig. 3).

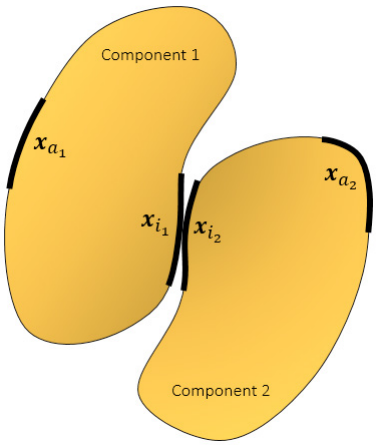


Fig. 3. Two mechanical components in contact through an extended contact interface. The black regions $\mathbf{x}_{i_j}$ and $\mathbf{x}_{a_j}$ denote the contact interface and active DoFs for the $j^{th}$ component.

Assume that each component is modeled by using the FE method. The DoFs vector of each component can be written as:

$$\mathbf{x}_j = \begin{Bmatrix} \mathbf{x}_{m_j} \\ \eta_{s_j} \end{Bmatrix}, \qquad \forall\ j = 1, 2 \tag{12}$$

where:

- $\mathbf{x}_{m_j}$ is the vector of $n_{m_j}$ master DoFs (i.e. the set of physical DoFs used to performed the dynamic analyses) of the $j^{th}$ component. $\mathbf{x}_{m_j}$ collects the set $\mathbf{x}_{i_j}$ of $n_{i_j}$ interface DoFs, and possibly the set $\mathbf{x}_{a_j}$ of $n_{a_j}$ active DoFs

($\mathbf{x}_{m_j} = [\mathbf{x}_{i_j}^T \ \mathbf{x}_{a_j}^T]^T$), so that $n_{m_j} = n_{i_j} + n_{a_j}$. Note that $\mathbf{x}_{a_j}$ could be empty if no other physical DoFs are required to perform the analyses except the interface ones.

- $\eta_{s_j}$ is the vector of $n_{s_j}$ modal DoFs. $\eta_{s_j}$ exists just if a CMS method (e.g. Craig-Bampton, Rubin) is applied to the FE matrices[2] (Gruber et al. (2016)). In this case the transformation matrix implementing the CMS reduction through a Galerkin projection process is denoted by $\mathbf{T}_j$.

In the most general case Eqn. 12 can be rewritten as:

$$\mathbf{x}_j = \begin{Bmatrix} \mathbf{x}_{i_j} \\ \mathbf{x}_{a_j} \\ \eta_{s_j} \end{Bmatrix}, \qquad \forall\ j = 1, 2 \tag{13}$$

The idea behind the GSI and MS reduction methods is that of representing the DoFs partitions $\mathbf{x}_{i_j}$ by means of a superposition of *interface modes*. If the interface modes are arranged as the columns of a *reduction matrix* $\Phi_{i_j k_j}$, the physical DoFs can be expressed by the following relationship:

$$\mathbf{x}_{i_j} \simeq \Phi_{i_j k_j} \eta_{k_j} \tag{14}$$

where the matrix $\Phi_{i_j k_j}$ has $n_{i_j}$ rows and $n_{k_j} \ll n_{i_j}$ columns, while $\eta_{k_j}$ is the vector of the corresponding $n_{k_j}$ modal coordinates. According to the result of Eqn. 14, Eqn. 13 becomes:

$$\begin{Bmatrix} \mathbf{x}_{i_j} \\ \mathbf{x}_{a_j} \\ \eta_{s_j} \end{Bmatrix} \simeq \begin{bmatrix} \Phi_{i_j k_j} & \mathbf{0} & \mathbf{0} \\ \mathbf{0} & \mathbf{I} & \mathbf{0} \\ \mathbf{0} & \mathbf{0} & \mathbf{I} \end{bmatrix} \begin{Bmatrix} \eta_{k_j} \\ \mathbf{x}_{a_j} \\ \eta_{s_j} \end{Bmatrix} = \mathbf{R}_j \mathbf{x}_{r_j}, \qquad \forall\ j = 1, 2 \tag{15}$$

where $\mathbf{R}_j$ is the global coordinates transformation matrix, while $\mathbf{x}_{r_j}$ is the new *reduced vector of generalized coordinates*. The reduced mass and stiffness matrices for the $j^{th}$ component can be found by applying the following Galerkin projection:

$$\mathbf{M}_j = \mathbf{R}_j^T \mathbf{T}_j^T \mathbf{M}_{FEM_j} \mathbf{T}_j \mathbf{R}_j \qquad \mathbf{K}_j = \mathbf{R}_j^T \mathbf{T}_j^T \mathbf{K}_{FEM_j} \mathbf{T}_j \mathbf{R}_j \qquad \forall\ j = 1, 2 \tag{16}$$

The matrices $\mathbf{M}$ and $\mathbf{K}$ of Eqn. 2 are finally obtained by assembling the matrices $\mathbf{M}_j$ and $\mathbf{K}_j$, while the damping matrix $\mathbf{C}$ is built by solving the eigenproblem defined by $\mathbf{M}$ and $\mathbf{K}$, assuming certain modal damping ratios $\zeta$.

Note that the smaller the number of retained interface modes $n_{k_j}$, the more effective the reduction of Eqn. 14. If the same reduction process is performed for the physical contact forces $\mathbf{F}_{c_n}^{(h)}$, the non-linear partition of Eqn. 7 gets the same dramatic reduction. In this way the non-linear solver operates on a smaller partition and less expensive computational efforts are required to evaluate the forced response of the structure.

[2] The FE mass and stiffness matrices are here denoted as $\mathbf{M}_{FEM_j}$ and $\mathbf{K}_{FEM_j}$ respectively

### 3.2. Gram-Schmidt interface reduction method

On the fulfillment of the partitioning of Eqn. 12 the undamped EQM of the $j^{th}$ component can be written as:

$$\begin{bmatrix} \mathbf{M}_{mm_j} & \mathbf{M}_{ms_j} \\ \mathbf{M}_{sm_j} & \mathbf{M}_{ss_j} \end{bmatrix} \begin{Bmatrix} \ddot{\mathbf{x}}_{m_j} \\ \ddot{\eta}_{s_j} \end{Bmatrix} + \begin{bmatrix} \mathbf{K}_{mm_j} & \mathbf{K}_{ms_j} \\ \mathbf{K}_{sm_j} & \mathbf{K}_{ss_j} \end{bmatrix} \begin{Bmatrix} \mathbf{x}_{m_j} \\ \eta_{s_j} \end{Bmatrix} = \begin{Bmatrix} \mathbf{f}_{m_j} \\ \phi_{s_j} \end{Bmatrix} \tag{17}$$

By solving the eigenproblem defined by the partitions $\mathbf{K}_{mm}$ and $\mathbf{M}_{mm}$ the full set of *characteristic constraint* modes is obtained (Castanier et al. (2001)). These can be arranged for increasing eigenvalues as the columns of the following modal matrix:

$$\Phi_{mm_j} = \begin{bmatrix} \varphi_{1_j} & \dots & \varphi_{m_j} \end{bmatrix} \tag{18}$$

The modal matrix of Eqn. 18 allows for a coordinate transformation involving all the master DoFs. If a coordinate transformation is desired just for a subset of $n_{i_j}$ physical DoFs, $\Phi_{mm_j}$ has to be partitioned as in the following equation:

$$\mathbf{x}_{m_j} = \begin{Bmatrix} \mathbf{x}_{i_j} \\ \mathbf{x}_{a_j} \end{Bmatrix} = \Phi_{mm_j} \begin{Bmatrix} \eta_{i_j} \\ \eta_{a_j} \end{Bmatrix} = \begin{bmatrix} \Phi_{ii_j} & \Phi_{ia_j} \\ \Phi_{ai_j} & \Phi_{aa_j} \end{bmatrix} \begin{Bmatrix} \eta_{i_j} \\ \eta_{a_j} \end{Bmatrix} \tag{19}$$

where $\eta_{i_j}$ and $\eta_{a_j}$ are two arbitrary set of modal coordinates with size $n_{i_j}$ and $n_{k_j}$ respectively. Previous studies on the GSI method proved that performing a *Gram-Schmidt* orthonormalization (Strang (1993)) on the columns of $\Phi_{ii_j}$ produces a good basis for the modal representation of the physical partitions $\mathbf{x}_{i_j}$. The size of $\mathbf{x}_{i_j}$ can be actually reduced if a modal truncation on the GSI modes is performed as suggested by the Eqn. 14.

#### 3.2.1. Application

The GSI method is here used to compute the non-linear forced response of a structure consisting of a *stator vane segment* connected to the corresponding *casing sector*. The assembly is characterized by two friction joints that exhibit a non-linear behavior: the interlocking and the hooks (Fig. 4).

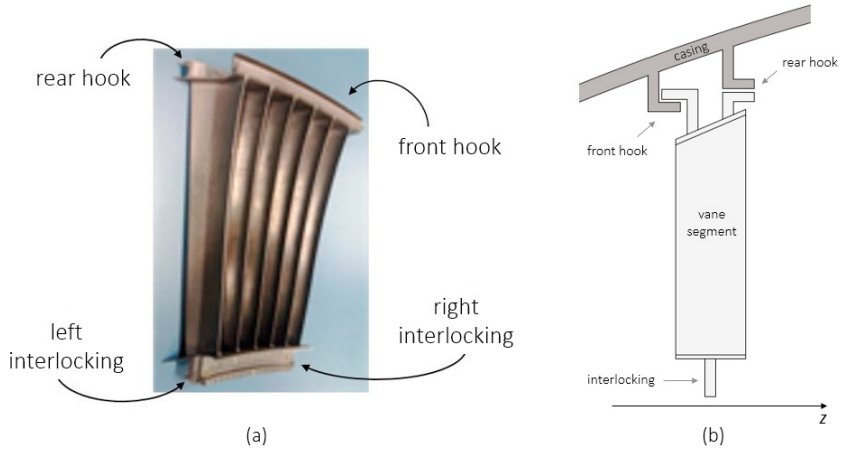


Fig. 4. (a) real vane segment of a low pressure turbine module for aeronautical applications; (b) schematic view of a stator vane segment connected at the casing by means of hook joints.

Although in the reality both joint typologies are active in terms of energy dissipation by friction, in this numerical application just the hook joints are considered. These in fact represent typical applications of lap joints with extended contact interfaces.

Due to the cyclic periodicity of the assembly the dynamic analyses were performed starting from the vane-casing sector FE model. A first reduced order model ($ROM_I$) was obtained by applying the Craig-Bampton CMS technique (CB-CMS). The total set of master DoFs retained in the reduction can be listed as follows:

- $n_{h_v} = n_{h_c} = n_h = 450$ DoFs at the hooks for the vane and casing. These sets DoFs are spread over the hooks contact interfaces.
- $n_i = 144$ DoFs at the interlocking joint. $n_i$ includes both the DoFs at the left and vane's interlocking.
- $n_a = 72$ DoFs at the blade and casing's outer surface.
- $n_c = 3080$ DoFs at the left and casing frontiers for the application of cyclic symmetry constraints.
- $n_k = 100$ modal coordinates corresponding to the reduced basis of fixed interface normal modes retained employed in the reduction.

The Tran method in combination with cyclic symmetry constraints (Tran (2001)) for a harmonic index 2, is applied in order to reduce the DoFs partitions $\mathbf{x}_{c_l}$ and $\mathbf{x}_{c_r}$ with $n_u = 100$ interface modal coordinates. The resulting ROM is such that mode shapes and natural frequencies of the starting FE model are captured with high accuracy (maximum percentage error on the natural frequencies $< 0.1\%$).

A new reduced order model (i.e. the $ROM_{II}$) was created by reducing the hooks DoFs by the GSI method. Previous studies on this reduction technique showed that an optimal set of modes used to reduce the contact interface is represented by a mix of *free* and *full-stick* GSI modes (Battiato et al. (2-2018)). The first are computed by leaving the interface DoFs "free", i.e. assuming no interaction between the neighboring contact interface. The second are computed by connecting the interface DoFs with spring elements having the same contact stiffnesses assumed for the contact element (Fig. 5).

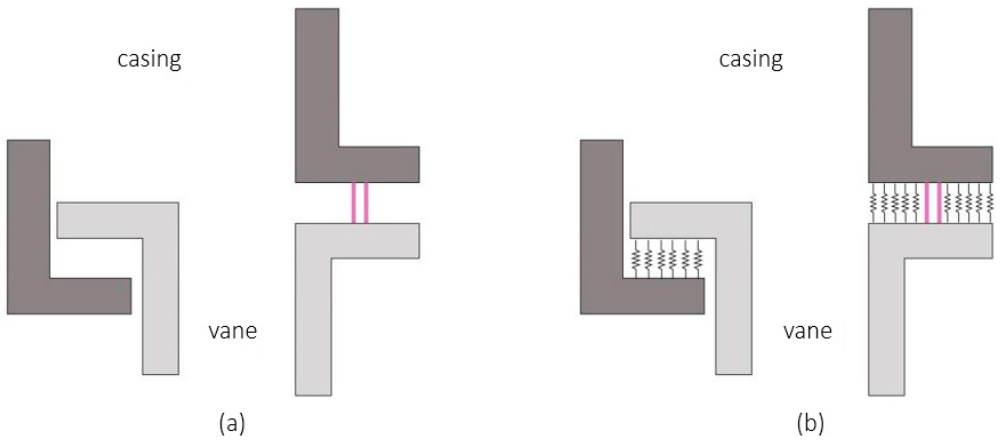


Fig. 5. (a) hooks in the free configuration; (b) hooks in the full-stick configuration.

The reason for that comes to the necessity of having a reduction basis suitable to represent the two possible extreme configuration of the contact interface: no contact (free) and full contact (full-stick).

In order to test the performances of the GSI method, a set of benchmark frequency response functions (FRFs) was obtained by solving the $ROM_I$. For validation purposes the normal preload at the interlocking was chosen in order to prevent any friction phenomena at the interlocking itself. The sensitivity parameter for each FRF is just represented by the normal preload $f_0$ at the front and rear hook joint. The black line plots in Fig. 6 show the trend of the benchmark FRFs when $f_0$ is varied. As expected, decreasing the value of $f_0$ makes the hook joints increasingly lose. This results in larger relative displacements at the contact interface which cause energy dissipation by friction and reduction of the vane vibration amplitude.

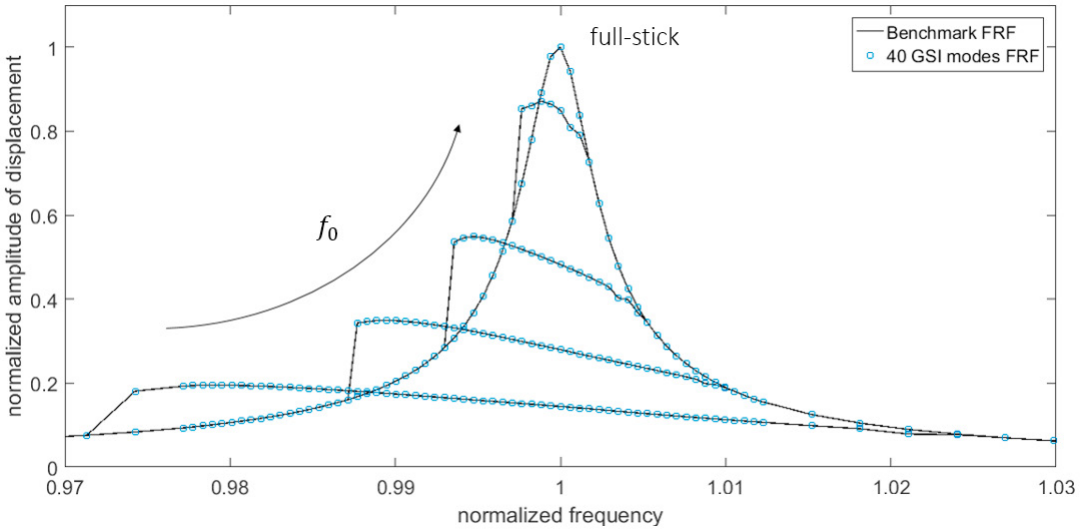


Fig. 6. Comparison between the FRFs obtained by using the $ROM_I$ (black line benchmark FRFs) and the $ROM_{II}$ (blue circle plots).

In the same figure the non-linear FRFs of the $ROM_{II}$ are compared with the benchmark ones. It can be noted that reducing the hooks interfaces with 40 GSI modes, i.e. 20 computed with the system in free condition and 20 with the system in full-stick condition, ensures a perfect matching of the FRFs. In fact, no significant differences can be found neither in terms of vibration amplitude nor in terms of resonance frequency.

The best performance of the $ROM_{II}$ are justified in terms of the size of the reduced model (1316 DoFs of the ROM without GSI reduction vs 436 DoFs of the GSI ROM) and time spent in the computation of each non-linear forced response (i.e. the calculation performed with the non-reduced contact interface was ~300 times slower than the calculation performed after the application of the GSI reduction technique). Note that the GSI reduction is particularly effective on the non-linear partition of the EQM, whose size decreased from 900 to 40.

### *3.3. Multi-Stage reduction method*

The MS reduction method was originally developed in order to solve the problem of coupling two or even more cyclic symmetric structures[3] having different number of sectors (D'Souza et al. (2011)). This is done by exploiting the "known" shapes of their vibrating modes. The modes exhibit a certain number of *nodal diameters H* (i.e. nodal lines along which the modal displacements are null), which allow describing the distribution of the displacements by the trigonometric functions $\sin(H\theta)$ and $\cos(H\theta)$ (Battiato et al. (2-2018)). Therefore, unlike the GSI method, the MS method does not require the computation of the interface modes since they are a priori known.

In order to understand how the interface DoFs $\mathbf{x}_{i_j}$ can be reduced, consider a stage composed by $N$ identical sectors (Fig. 7 (a)). The FE model of the sector representative of the whole stage geometry is constructed so that groups of nodes at its interface have the same angle in a cylindrical coordinate system which is aligned with the axis of the stage itself. These groups of nodes are referred to as *radial line segments* (Battiato et al. (2-2018)), and $Z$ of them exist within each sector (Fig. 7 (b)). Therefore, $NZ$ is the total number of radial line segments at the stage interface. The number of DoFs per radial line segment is $n_l$.

[3] The cyclic symmetric structure are here often denoted as *stages*. This term comes from the usual field of application, i.e. the turbomachinery field.

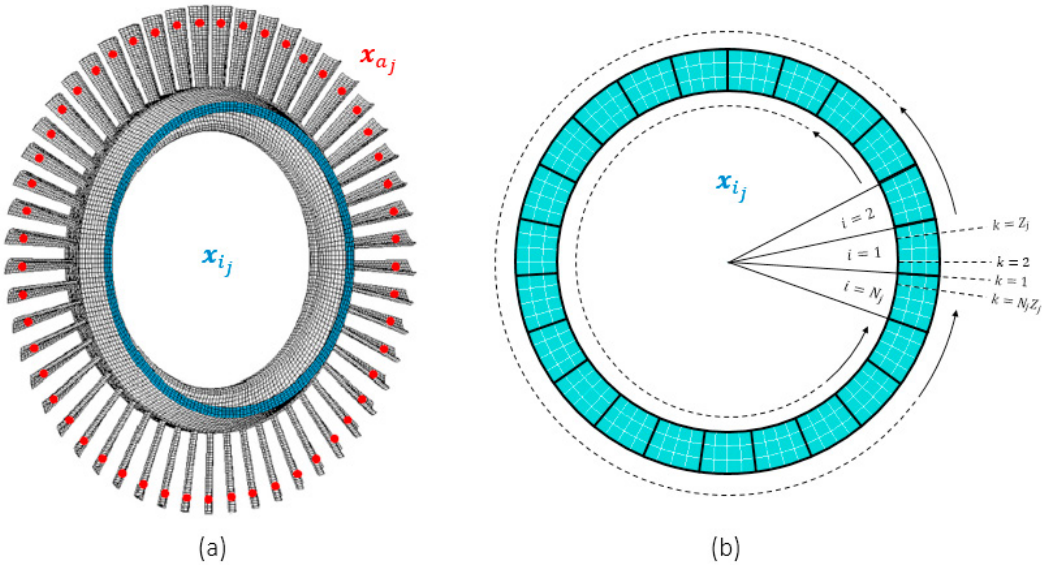


Fig. 7. (a) interface and active DoFs for a bladed disk; (b) inter-stage boundary of a cyclic symmetric stage. Sectors and radial line segments are denoted by $i$ and $k$ respectively.

The vector $\mathbf{x}_{i_j}$ can then be partitioned as follows:

$$\mathbf{x}_{i_j} = \begin{Bmatrix} \mathbf{x}_{R1_j} \\ \mathbf{x}_{R2_j} \\ \vdots \\ \mathbf{x}_{RNZ_j} \end{Bmatrix} \tag{20}$$

where the subscript $R$ stands for "radial line segment". The motion $\mathbf{x}_{Rk_j}$ of the $k^{th}$ radial line segment of the $j^{th}$ stage can be expressed by using the following relationship (Battiato et al. (2-2018)):

$$\mathbf{x}_{Rk_j} = \frac{1}{\sqrt{NZ}}\mathbf{a}^0_{i_j} + \sqrt{\frac{2}{NZ}}\sum_{h=1}^{\tilde{R}-1}\mathbf{a}^h_{i_j,c}\cos[(j-1)\varphi_k] + \sqrt{\frac{2}{NZ}}\sum_{h=1}^{\tilde{R}-1}\mathbf{a}^h_{i_j,s}\sin[(j-1)\varphi_k] + \frac{1}{\sqrt{NZ}}(-1)^{j-1}\mathbf{a}^{\tilde{R}} \tag{21}$$

where $\varphi_k = 2\pi k/(NZ)$, $\mathbf{a}_{i_j}$ denote a vector of interface spatial Fourier coefficients with subscripts $c$ or $s$ identifying the cosine and sine components respectively and $\tilde{R} = NZ/2$ if $NZ$ is even or $\tilde{R} = (NZ-1)/2$ if $NZ$ is odd. The last term Eqn. (21) does not exist if $NZ$ is odd. If the spatial Fourier coefficients are grouped as follows:

$$\mathbf{a}_{i_j} = \{(\mathbf{a}^0_{i_j})^T, (\mathbf{a}^1_{i_j,c})^T, (\mathbf{a}^2_{i_j,c})^T, \ldots, (\mathbf{a}^{\tilde{R}-1}_{i_j,c})^T, (\mathbf{a}^{\tilde{R}}_{i_j,c})^T, (\mathbf{a}^{\tilde{R}-1}_{i_j,s})^T, \ldots, (\mathbf{a}^2_{i_j,s})^T, (\mathbf{a}^1_{i_j,s})^T\}^T \tag{22}$$

the interface DoFs can be written as:

$$\mathbf{x}_{i_j} = (\mathbf{F}_{NZ,NZ} \otimes \mathbf{I}_{n_l})\mathbf{a}_{i_j} = \mathcal{F}\mathbf{a}_{i_j} \tag{23}$$

where $\mathbf{I}_{n_l}$ is the identity matrix of size $n_l$ and $\mathbf{F}_{NZ,NZ}$ is the $NZ \times NZ$ real valued Fourier matrix (Castanier et al. (2016)). Eqn. 23 represents a pure coordinate transformation and does not introduce any reduction of the interface DoFs $\mathbf{x}_{i_j}$. However, a strong reduction of the set $\mathbf{a}_{i_j}$ can be achieved by just retaining the columns of $\mathbf{F}_{NZ,NZ}$ corresponding to the mode shapes having the desired number of nodal diameters $H$. All the other mode shapes are neglected. If $\Sigma$ is the set of harmonic indexes corresponding to the EO exciting the structure (Eqn. 1), the coordinate transformation of Eqn. 23 becomes a reduction just if the $\Sigma$ columns of $\mathbf{F}_{NZ,NZ}$ are retained.

### *3.3.1. Application*

The MS reduction method is here used to compute the non-linear forced response of a multi-stage system with friction contacts at the flange joint. The structure consists of two different bladed disks with the same number $N$ of sectors ($N = 50$ for each disks, Fig. 8).

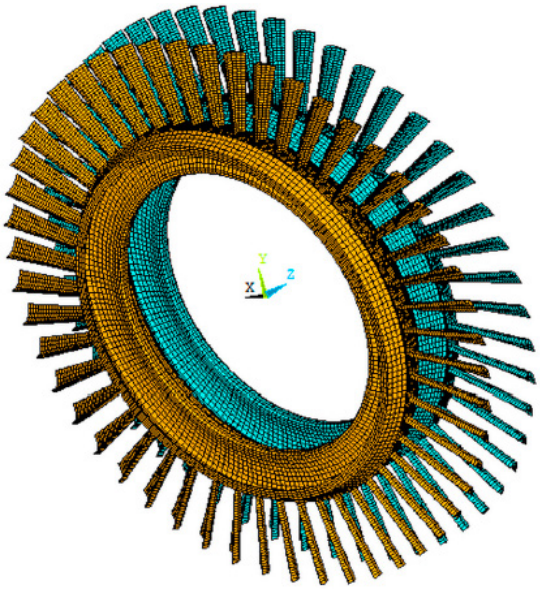


Fig. 8. Multi-stage bladed disk FE model.

The FE models of the two stages were generated in ANSYS by repeating the FE models of the fundamental sectors $N$ times around the $z$-axis. The stages 1 and 2 consist of 43200 and 40300 4-node brick elements with 42250 and 38900 nodes respectively. The material properties were chosen according to the standard values of the steel: Young's modulus $E = 210$ GPa, Poisson's ration $\nu = 0.33$ and density $\rho = 7800$ kg/m$^3$. For both stages the number of radial line segments per sector is $Z = 4$. All the radial line segments have five equally spaced nodes, meaning that the two stages have perfectly matching meshes at the contact interface.

A first reduced order model was obtained by applying the CB-CMS method to the stages. For each of them the set of interface and active DoFs $\mathbf{x}_{i_j}$ and $\mathbf{x}_{a_j}$ were retained as master. $\mathbf{x}_{i_j}$ represents the vector of DoFs of the nodes lying on the medium radius circumference of the $j^{th}$ stage contact surface, while $\mathbf{x}_{a_j}$ was defined by selecting one node per blade in the middle of the blades' airfoils (Fig. 7 (a)). In addition the first 200 fixed-interface normal modes were employed in the reduction of the two stages, yielding two *CB*-CMS ROMs with 950 DoFs each[4]. The reduced order model resulting from the CB-CMS reduction of the two stages is here denoted as a ROM$_I$.

The multi-stage system was assumed to be excited by two clocked EO = 2 traveling waves. Therefore, a second reduced order model, i.e. the ROM$_{II}$, was obtained by just retaining the columns of the Fourier matrix corresponding to the harmonic index $H = 2$ (Eqn. 1 for $z = 0$). By looking at the Table 1 it can be noted how a strong reduction of the interface DoFs is achieved when the coordinate transformation of Eqn. 23 is applied.

[4] For reference, the first 200 natural frequencies of the *CB*-CMS ROMs are within the 0.3% of the corresponding FE natural frequencies.

Table 1. Sizes of the DoFs partitions for the reduced order models $ROM_I$ and $ROM_{II}$.

| ROM | # interface DoFs | # active DoFs | # CB-CMS modal coordinates | # total DoFs |
|---|---|---|---|---|
| $ROM_I$ | 1000 | 300 | 400 | 1700 |
| $ROM_{II}$ | 12 | 300 | 400 | 712 |

By solving non-linear reduced order models $ROM_I$ and $ROM_{II}$, the forced response for the stage 1 and 2 are obtained.(Figs. 9 and 10).

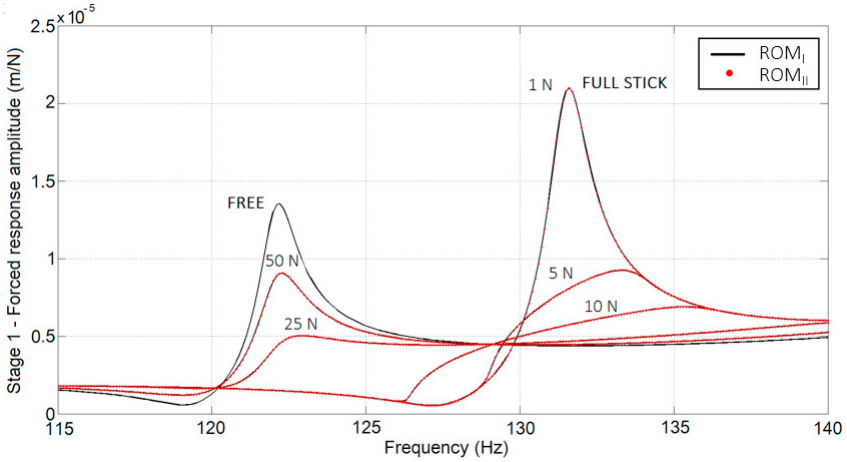


Fig. 9. Normalized forced responses of the stage 1: $ROM_I$ vs $ROM_{II}$.

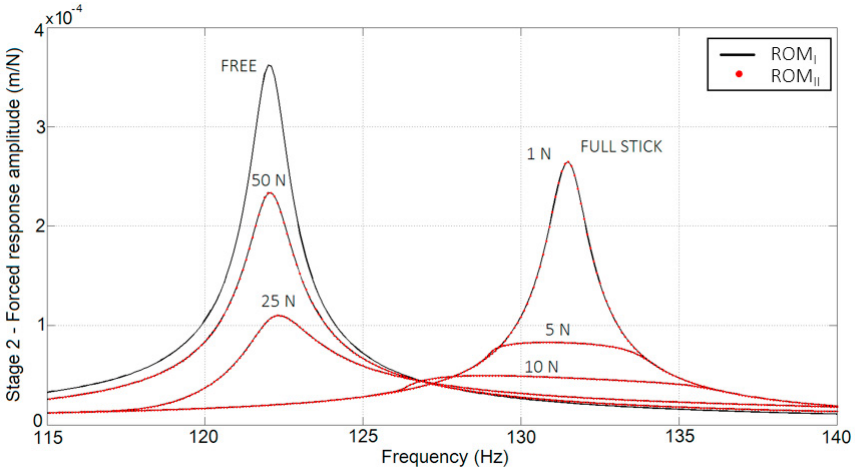


Fig. 10. Normalized forced responses of the stage 2: $ROM_I$ vs $ROM_{II}$.

It is possible to observe the typical behavior of friction joints where the *full stick* condition occurs for small value of $F_0$ ($F_0$ = 1N). By increasing the excitation amplitude slip occurs, and the peak response decreases and shifts towards the *free* response where no friction is present. Similar trends were also found in Battiato et al. (1-2018) meaning that the flange can be considered as a component that can be designed in order to be an important and optimal source of damping.

Figs. 9 and 10 clearly shows the perfect match between the non-linear forced responses computed by using the $ROM_I$ and $ROM_{II}$. These results make the $ROM_{II}$ preferable when non-linear calculation have to be performed. The

best performance of the $ROM_{II}$ can be justified in terms of size of the model (1700 DoF of the $ROM_I$ vs 712 DoF of the $ROM_{II}$) and time spent in the computation of each nonlinear forced response ($\sim$ 890 s for the $ROM_I$ vs $\sim$ 30 s for the $ROM_{II}$). The efficiency of the MS reduction method lies on the high compression achieved for the interface DoFs (i.e. 1000 for the $ROM_I$ vs 12 for the $ROM_{II}$).

## 4. Conclusions

The current trend in the design process is the simulation of large complex systems made by a large number of components. The ambitious task of the whole system simulation relies, first, on a suitable tuning of the single components FE model participating to the full structure and, second, on a suitable modeling of the interface between components. When such interfaces can not be considered as localized with respect to the physical domain of the components, classic reduction techniques are no more efficient in terms of computational time. For this reason, dedicated reduction techniques for the contact interfaces have to be developed in particular when the uncertainty of loose contacts is taken into account. In this paper a method to overcome the long computations of the frictionally damped non-linear response of jointed structures with large contact interfaces is presented. It is based on the idea of modal reduction of the interface degrees of freedom by using suitably defined bases of interface modes. To this aim two novel reduction techniques are introduced: the Gram-Schmidt Interface method and the Multi-stage method. The first is proved to be effective for contact interfaces having a generic geometry, while the second is appositely developed for circular interfaces. Results show high accuracy in the prediction of the non-linear forced response of structure with lap joints with a remarkable reduction of the computational cost without loosing the accuracy of the benchmarks solution.

## References

Battiato, G., Firrone, C. M., Berruti, T. M., & Epureanu, B. I., 2016. Reduced order modeling for multi-stage coupling of cyclic symmetric structures. In International Conference on Noise and Vibration Engineering and International Conference on Uncertainty in Structural Dynamics (ISMA/USD), Leuven, Belgium, Sept (pp. 19-21).

Battiato, G., Firrone, C. M., Berruti, T. M., & Epureanu, B. I., 2018. Reduced order modeling for multistage bladed disks with friction contacts at the flange joint. Journal of Engineering for Gas Turbines and Power, 140(5), 052505.

Battiato, G., Firrone, C. M., Berruti, T. M., & Epureanu, B. I., 2018. Reduction and coupling of substructures via GramSchmidt Interface modes. Computer Methods in Applied Mechanics and Engineering, 336, 187-212.

Battiato, G., Firrone C. M., 2018. Reduced order modeling for forced response prediction of structures with large contact interfaces. Proceedings of ISMA Conference, Leuven, Belgium.

Cameron, T. M., & Griffin, J. H., 1989. An alternating frequency/time domain method for calculating the steady-state response of nonlinear dynamic systems. Journal of applied mechanics, 56(1), 149-154.

Cardona A., Lerusse A., & Geradin M., 1998. Fast Fourier Nonlinear Vibration Analysis. Computational Mechanics, 22(2), 128-142.

Castanier M.P., Ottarsson G. & Pierre C., 1997. A reduced order modeling technique for mistuned bladed disks. Journal of Vibration and Acoustics, 119(3), 439-447.

Castanier M.P., & Pierre C., 2006. Modeling and analysis of mistuned bladed disk vibration: current status and emerging directions. Journal of Propulsion and Power, 22(2), 384-396.

Castanier M. P., Yung-Chang T., & Pierre C., 2001. Characteristic constraint modes for component mode synthesis. AIAA journal, 39(6), 1182-1187.

D'Souza K.X., Epureanu B.I., 2012. A statistical characterization of the effects of mistuning in multistage bladed disks. Journal of Engineering for Gas Turbines and Power, 134(1), 012503.

Firrone C. M., Battiato G., & Epureanu B. I., 2018. Modeling the Microslip in the Flange Joint and Its Effect on the Dynamics of a Multistage Bladed Disk Assembly. Journal of Computational and Nonlinear Dynamics, 13(1), 011011.

Firrone C. M., Berruti T. M., & Gola M. M., 2013. On force control of an engine ordertype excitation applied to a bladed disk with underplatform dampers. Journal of vibration and acoustics, 135(4), 041103.

Firrone C. M., & Zucca S., 2011. Modelling friction contacts in structural dynamics and its application to turbine bladed disks. Numerical Analysis-Theory and Application, 301-334.

Gruber F.M., & Rixen D.J., 2016. Evaluation of substructure reduction techniques with fixed and free interfaces. StrojniÅki vestnik-Journal of Mechanical Engineering, 62(7-8), 452-462.

Holzwarth P., & Eberhard P., 2015. Interface reduction for CMS methods and alternative model order reduction. IFAC-PapersOnLine, 48(1), 254-259.

Krack M., Panning L., Wallaschek J., Siewert C., & Hartung A., 2013. Reduced order modeling based on complex nonlinear modal analysis and its application to bladed disks with shroud contact. Journal of Engineering for Gas Turbines and Power, 135(10), 102502.

Kuether R. J., Allen M. S., & Hollkamp J. J., 2017. Modal substructuring of geometrically nonlinear finite element models with interface reduction. AIAA Journal, 1695-1706.

Lassalle M., & Firrone C. M., 2016. Nonlinear Forced Response of a Stator Vane with Multiple Friction Contact Using a Coupled Static/Dynamic Approach. VII European Congress on Computational Methods in Applied Sciences and Engineering Crete Island, Greece, June.

Petrov E. P., & Ewins D. J., 2007. Advanced modeling of underplatform friction dampers for analysis of bladed disk vibration. Journal of Turbomachinery, 129(1), 143-150.

Poudou O., & Pierre C., 2003. Hybrid frequency-time domain methods for the analysis of complex structural systems with dry friction damping. In 44th AIAA/ASME/ASCE/AHS/ASC Structures, Structural Dynamics, and Materials Conference (p. 1411).

Sanliturk K. J., Ewins D. J., & Stanbridge A. B., 2001. Underplatform dampers for turbine blades: theoretical modeling, analysis, and comparison with experimental data. Journal of Engineering for Gas Turbines and Power, 123(4), 919-929.

Schwingshackl C. W., Petrov E. P., & Ewins D. J., 2012. Effects of contact interface parameters on vibration of turbine bladed disks with underplatform dampers. Journal of Engineering for Gas Turbines and Power, 134(3), 032507.

Strang G., 1993. Introduction to linear algebra (Vol. 3). Wellesley, MA: Wellesley-Cambridge Press.

Tran D. M., 2001. Component mode synthesis methods using interface modes. Application to structures with cyclic symmetry. Computers & Structures, 79(2), 209-222.

Yang, B. D., Chu, M. L., & Menq, C. H., 1998. Stickslipseparation analysis and non-linear stiffness and damping characterization of friction contacts having variable normal load. Journal of Sound and vibration, 210(4), 461-481.

Zucca S., Firrone C., & Gola M., 2012. Numerical assessment of friction damping at turbine blade root joints by simultaneous calculation of the static and dynamic contact loads. Nonlinear Dynamics, 67(3), 1943-1955.